Carbohydrate Polymers 92 (2013) 200–205

Contents lists available at SciVerse ScienceDirect

Carbohydrate Polymers

journal homepage: www.elsevier.com/locate/carbpol

Structure and protective effect on UVB-induced keratinocyte damage of fructan from white garlic

Jinling Chen [a], Kit leong Cheong [a], Ziliang Song [a], Yujie Shi [b], Xuesong Huang [a,*]

[a] Department of Food Science and Engineering, Jinan University, Guangzhou 510632, China
[b] Department of Dermatology, The Second Affiliated Hospital of Guangzhou Medical University, Guangzhou 510260, China

ARTICLE INFO

Article history:
Received 21 June 2012
Received in revised form 29 August 2012
Accepted 25 September 2012
Available online 3 October 2012

Keywords:
Garlic
Fructan
1-Kestose
Structure
NMR
UVB

ABSTRACT

The fructose polymer fructan was extracted from white garlic and fractionated using DEAE cellulose 52 and Sephadex G-100 columns to characterize its chemical composition and protective effect against ultraviolet radiation b (UVB) induced human keratinocyte (HaTaC) damage. Gel permeation chromatography, high performance anion exchange chromatography, infrared spectroscopy and 1D and 2D nuclear magnetic resonance spectroscopy were used to determine the chemical composition and functional characteristics of the garlic fructan (GF). GF was a homogeneous polysaccharide with a molecular weight of 4.54×10^3 Da. It was a member of the 1-kestose family, and it was composed of fructose and glucose at a ratio of 14:1. The main chain of GF was composed of (2 → 1)-β-D-fructopyranose linked to a terminal (2 → 1)-α-D-glucopyranose at the non-reducing end and a (2 → 6)-β-D-fructopyranose branched chain. The degree of polymerization was 28. Preliminary tests described herein indicated that GF may be effective in protecting HaTaC from UVB-induced damage.

1. Introduction

Natural polysaccharides have attracted considerable attention in both biochemical and medical research due to their unique bioactivities and chemical structures (Yang & Zhang, 2009). For example, polysaccharides with (1 → 3)-linked-glucose backbones (Zeng, Zhang, Gao, Jia, & Chen, 2012), (1 → 6)-linked-α-D-glucopyranosyl and (1 → 2,6)-linked-α-D-glucopyranosyl residues (Luo, Sun, Wu, & Yang, 2012), (1 → 5)-linked arabinose (Tong, Liang, & Wang, 2008), and (1 → 3)-linked-β-D-Galp main chains (Cipriani et al., 2006) are reported to account for antioxidative, immunostimulatory, antidiabetic, antiulcerative effects, respectively. In particular, natural polysaccharides play an important role as free radical scavengers in the prevention of oxidative damage, and they can be exploited as novel antioxidants. Therefore, the discovery and evaluation of polysaccharides from plant materials for use as functional foods or medicines are an important new area of research.

Garlic (*Allium sativum* L.) is a herbaceous perennial plant that contains 23% fructan (w/w) on a fresh garlic basis or >75% (w/w) on a dry garlic basis (Praznik, Huber, & Cieslik, 2004). The fructan isolated from garlic is a series of homologous oligo- and polysaccharides, ranging in molecular weight from 1000 Da to 10,000 Da, binding with a degree of polymerization (DP) as high as 58 (Baumgartner, Dax, Praznik, & Falk, 2000; Chandrashekar, Harish Prashanth, & Venkatesh, 2011; Losso & Nakai, 1997). The basic structure of garlic fructan (GF), as reported by Baumgartner et al. (2000) and Chandrashekar et al. (2011), was a β-2,1-linked fructoside, however, they had different opinions on the α-D-glucopyranosyl linkage. Baumgartner et al. (2000) suggested that α-D-glucopyranosyl was linked to β-D-fructopyranose at the (1 → 6) position, based on gas chromatography–mass spectrometry evidence of the presence of one residue of 6-O-linked α-D-glucopyranosyl, and Chandrashekar et al. (2011) showed that an α-D-glucopyranosyl residue was linked to a terminal (2 → 1) linkage at the non-reducing end. These inconsistencies should be resolved by 2D NMR, but to date, this has not been accomplished. Therefore, it is necessary to elucidate the actual structure of GF using several different analytical methods, including 2D NMR spectral analysis.

Several pharmacological effects have been attributed to GF, including anticholera toxin B, anticytotoxin, and immunoregulatory activity (Chandrashekar et al., 2011; Politi et al., 2006; Tsukamoto, Okamoto, Inanaga, & Karasaki, 2008). GF may also enhance *Lactobacillus* spp. fermentation (Huang & Chen, 2011). However, the efficacy of GF on damage induced by ultraviolet radiation b (UVB) at wave length from 275 to 320 nm (Chen, Cao, & Song, 2010) has not been studied. Free radical induced peroxidation of membrane lipids leads to cell damage and subsequent tissue injury (Hsiao et al., 2003). As well, over exposure to UVB from the sun adversely effects human health by forming detrimental photoproducts, arresting the cell cycle, inducing photoaging, and causing inflammation (Kippenberger et al., 2001; Liu, Mizu, & Yamauchi,

* Corresponding author. Tel.: +86 020 85226630; fax: +86 020 85226630.
E-mail address: thxs@jnu.edu.cn (X. Huang).

0144-8617/$ – see front matter © 2012 Elsevier Ltd. All rights reserved.
http://dx.doi.org/10.1016/j.carbpol.2012.09.068

2007). Shi, Yan, Li, and Huang (2008) reported that GF scavenged superoxide anion and hydroxyl radicals. Therefore, it is of interest to investigate the role of GF in inhibiting proliferative activity and apoptosis in UVB-irradiated human keratinocyte cells (HaCaT).

The intent of this work was to isolate GF from white garlic by extracting with ethanol and then determined its structural characteristics, including its MW and monosaccharide composition, using infrared spectroscopy (IR), and 1D and 2D nuclear magnetic resonance spectroscopy (NMR). In addition, the effect of GF on UVB exposed HaCaT cells were estimated by studying cell activation and the cell cycle. The 30 mJ/cm^2 UVB was selected based on the results of Sitailo, Tibudan, and Denning (2002).

2. Materials and methods

2.1. Materials and reagents

White garlic from Shandong province was purchased from a local market in Guangzhou. Dextrans T-5, T-20, T-40, T-200, T-270, T-2000, glucose, arabinose, galactose, rhamnose, mannose and fructose were purchased from Sigma–Aldrich (MO, USA). DEAE cellulose 52 and Sephadex G-100 were obtained from Whatman and Pharmacia (Shanghai, China), respectively. Human keratinocyte cells (HaCaT) were obtained from China center for type culture collection. Ethylene diamine tetraacetic acid (EDTA), Dulbecco's modified eagle medium (DMEM), trypsinase, dimethyl sulfoxide (DMSO), and 3-(4,5-dimethylthiazol-2-yl)-2,5-diphenyl tetrazolium bromide (MTT) were products of Gibco-BRL (Gaithersbrug, MD, USA). Fetal bovine serum (FBS) was purchased from Hangzhou sijiqing biological engineering materials Co., Ltd. The UVB light source (8 W, 305 nm) and the Bio-sun lamp came from the Beijing lighting research institute. Flow cytometry was from Becton dickinson and company limited. All other regents and chemicals used were of analytical grade.

2.2. Separation and purification of GF

White, skinless garlic cloves were boiled at 100 °C for 20 min to inhibit the activity of endogenous enzymes, and they were then grounded with 1:1 (v/v) distilled water and broken into pieces. The suspensions were extracted thrice by the addition of ethanol to a final concentration of 30% (v/v). Following centrifugation (3500 × *g*, 20 min), supernatant was precipitated by the addition of ethanol to a final concentration of 80% (v/v) to remove pigments, monosaccharides, oligosaccharides and other micromolecule materials. Precipitates were collected by centrifugation (3500 × *g*, 20 min), washed successively with 80% (v/v) ethanol, and solubilized in distilled water to obtain crude GF. The crude polysaccharide solution was subjected to DEAE cellulose 52 column (2.5 cm × 60 cm) and eluted with distilled water at a flow rate of 1.0 ml/min. Eluted fractions were collected and analyzed for carbohydrate content based on the phenol–sulfuric acid method at 490 nm absorbance (Masuko et al., 2005). Finally, the eluted fractions were concentrated and lyophilized. The fractions were further purified on a Sephadex G-100 column (2.5 cm × 60 cm) using distilled water at a flow rate of 0.5 ml/min and lyophilized to obtain pure GF. The purity of the GF was determined by high performance gel permeation chromatography (HPGPC), which was preformed on a Shimadzu LC-20AT high performance liquid chromatograph (HPLC, Japan) with a PolySep-GPC-P4000 column (7.8 mm × 300 mm, Guangzhou Feiluomen scientific instrument Ltd.) and SPD-M20A refractive index detector (RID). Column temperature was held constant at 20 °C. The injection volume was 30 μl, and the eluent was pure water at 0.5 ml/min.

2.3. Molecular weight determination

The MW of GF was determined by HPGPC. The detailed operation conditions were as mentioned in Section 2.2. The calibration curve for the MW determination was constructed using dextrans T-5, T-20, T-40, T-200, T-270, T-2000 and glucose, and all measurements were obtained in triplicate.

2.4. Analysis of monosaccharide composition

A high performance anion exchange chromatography-pulsed amperometric detector (HPAEC) was used for the identification and quantification of the monosaccharide. One hundred milligrams of GF were hydrolyzed with 2 ml of 0.05 M sulfuric acid at 100 °C for 8 h. The hydrolyzed polysaccharide was mixed with $BaCO_3$ to adjust the pH to neutrality, and it was then passed through Millipore filters (0.45 μm and 0.2 μm) before analysis. The sample was diluted 10,000-fold for detection on an HPAEC ICS-2500 (Dionex Corporation, USA) with a CarboPac PA-10 (4 mm × 250 mm) analytical column and a CarboPac PA-10G (4 mm × 50 mm) protective column. The temperature of the column was 30 °C, and the injection volume was 25 μl. The eluent was 250 mM NaOH at 0.2 ml/min. Arabinose, galactose, glucose, mannose, rhamnose and fructose were used as standard monosaccharides. Triplicate determinations were made.

2.5. IR spectroscopy of GF

The IR of GF was recorded using an EQUINOX 55 Fourier counter exchange absorption infrared spectrometer (Bruker, Germany) over a range of 400–4000 cm^{-1}. The sample was analyzed as KBr pellet.

2.6. NMR spectroscopy of GF

To obtain NMR data quickly, 150 mg GF were dissolved in D_2O at room temperature. Both ^{1}H and ^{13}C spectrums were recorded on a Bruker Avance 400 MHz NMR spectrometer (Germany). The spectrum of ^{1}H, ^{13}C, ^{1}H/^{1}H correlation spectroscopy (COSY), heteronuclear single-quantum coherence (HSQC) and heteronuclear multiple-bond correlation (HMBC) experiments were conducted at 30 °C.

2.7. Cell culture

HaCaT cells were grown in DMEM containing 10% (v/v) FBS at 37 °C humidified atmosphere of 5% (v/v) CO_2. The cells were trypsinized with 0.5% (w/w) trypsin and 0.03% (w/w) EDTA, and subcultured when the population reached 90–95% confluency.

2.8. Cell proliferation determination by MTT assay

The viability levels of HaCaT cells were determined by the ability of mitochondria to convert MTT to insoluble formazan product. Briefly, HaCaT (100 μl, 1 × 10^5 cells/ml) was cultured with GF (0, 250, 500, 1000, 2000, 4000, 8000 μg/ml) in 96-well plates and incubated as described in Section 2.7. Following incubation for 12 h, the cells were washed with PBS and stimulated by UVB radiation (30 mJ/cm^2) in PBS. Immediately following irradiation, the cells were treated with different concentrations of GF as mentioned above in new serum free medium and incubated for 12 h at 37 °C in a humidified atmosphere of 5% (v/v) CO_2. The supernatant was removed, and 10 μl of 5 mg/ml MTT reagent (MTT dissolved in 0.1 M Tris-buffered saline; filtered) were added to each well, followed by incubation for 4 h. After removal of unconverted MTT, the amount of formazan in the cells was determined by adding DMSO and

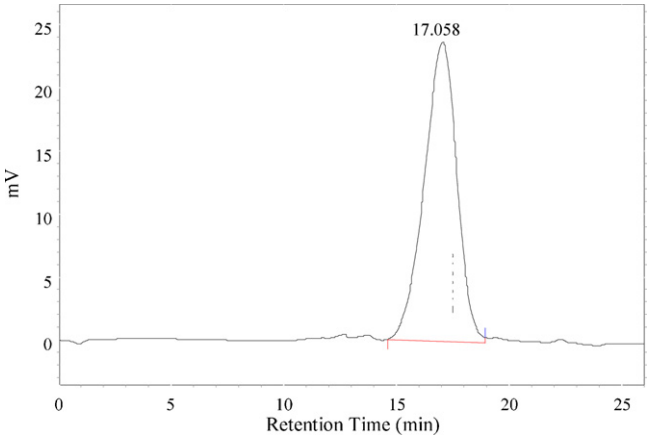

Fig. 1. Profile of GF in HPGPC.

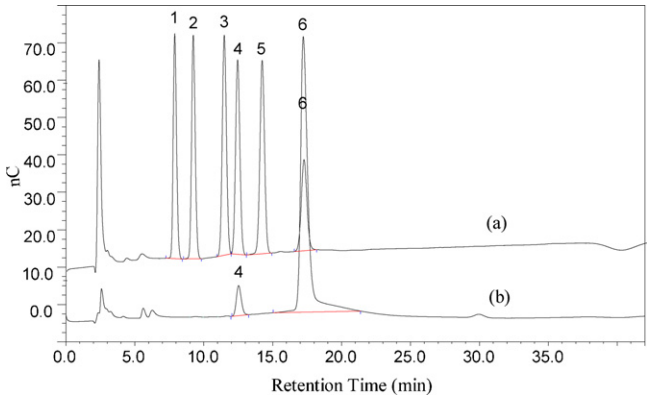

Fig. 2. HPAEC chromatogram profile of standard monosaccharide mixture solution (a) and hydrolysate of GF (b). (a) Peak identity: (1) Rha (rt: 7.802); (2) Ara (rt: 9.135); (3) Gal (rt: 11.385); (4) Glc (rt: 12.352); (5) Man (rt: 14.135); (6) Fru (rt: 17.168). (b) Peak identity: (4) Glc (rt: 12.534); (6) Fru (rt: 17.217).

measuring optical density (OD) at a wavelength of 570 nm using a microplate reader. Relative cell viability was calculated as the percent viability of untreated cells that were designated to be the control cells.

2.9. Cell cycle analysis by flow cytometry

HaCaT (1 ml, 1×10^5 cells/ml) was grown with GF (0, 250, 500, 1000, 2000, 4000, 8000 μg/ml) in 6-well plates and incubated as described in Section 2.7. Cells were exposed to 30 mJ/cm^2 of UVB and immediately treated with different concentrations of GF as mentioned above in new serum free medium for 12 h. The supernatant was removed, and the cell pellet was washed twice with PBS, followed by trypsinization. The cells were scrapped into a centrifuge tube. After centrifugation at 1000 rpm for 5 min, the cell pellet was washed twice with PBS at 4 °C, and resuspended in 70% (v/v) ethanol at 4 °C for 30 min. This was followed three washes with PBS. Finally, the cells were stained with propidium iodide (PI) and incubated in the dark for 30 min. The sub-G1 DNA content of the cells after PI staining was determined by flow cytometry.

2.10. Statistical analysis

Data were expressed as the mean ± SD (standard deviation) ($n = 3$ or 6). Data from all the bioassays were evaluated by analysis of variance and $p < 0.05$ was considered to be significant.

3. Results and discussion

3.1. Preparation and structural analysis

The crude water-soluble polysaccharide from white garlic was separated and purified by DEAE cellulose 52 and Sephadex G-100 gel filtration chromatogram. Purified GF was obtained with a yield of 6.15% (w/w), based on dry matter, and it appeared as a white powder. It showed a single, symmetrical sharp peak on the HPGPC (Fig. 1) indicated that it was a homogeneous polysaccharide, which had been removed from a mixture of pigments, monosaccharides, oligosaccharides, polysaccharides, protein and other micromolecule materials. Its MW was estimated to be 4.54×10^3 Da by HPGPC, based on the calibration curve that had been established using standard dextrans and glucose. It also responded negatively to the Bradford test and showed no absorption at 280 nm in the UV spectrum indicated the absence of protein. Quantitative analysis results using HPAEC following GF hydrolysis revealed that GF was composed of fructose and glucose (Fig. 2) at a ratio of 14:1. These data indicated that fructose was the predominant monosaccharide present.

As shown in Fig. 3, the different absorption bands from the IR analysis were assigned as previously described (Chen et al., 2012; Nguyen, Do, Nguyen, Pham, & Nguyen, 2011). For GF, a broad band centered at 3447.1 cm^{-1} was attributable to —OH groups. An intense band centered at 2927.5 cm^{-1} was due to the —CH stretching and was characteristic of polysaccharides. The absorption band centered at 1639 cm^{-1} was caused by —OH flexural vibration of the polysaccharide. The absorption band centered at 1461 cm^{-1} assigned to —CH (O—CH_2) flexural vibrations. The group of bands that extended from 1068 to 1025 cm^{-1} corresponded to C—O stretching vibrations. Characteristically, the bands at 1000–800 cm^{-1} suggested the presence of furanose residue in GF. The absorption bands centered at 933.6 cm^{-1} and 810.0 cm^{-1} were due to the existence of fructose with β-type glycosidic bond, which was in good agreement with the results of the HPAEC analysis. All the absorption bands listed above were IR characteristic peaks of GF.

The structural features of GF were further identified by 1D and 2D NMR spectrum. The ^{1}H NMR spectrum (Fig. 4a) showed one anomeric H at δ 5.31 ppm which indicated that the glucose was α-D-Glc. Other sugar protons were in the region of δ 3.10–4.20. The ^{13}C NMR spectrum (Fig. 4b) for the polysaccharide mainly contained signals for anomeric carbons at δ 90–105, and sugar ring carbons linked to oxygen in the region of δ 60–82 (Zhang, Xiao, Deng, He, & Sun, 2012).

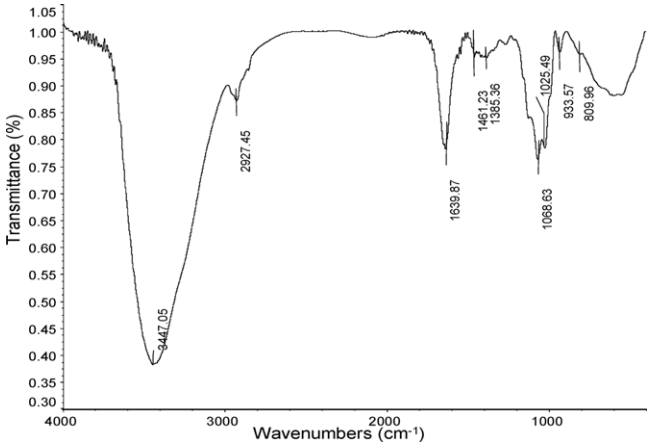

Fig. 3. Infrared spectrum of GF.

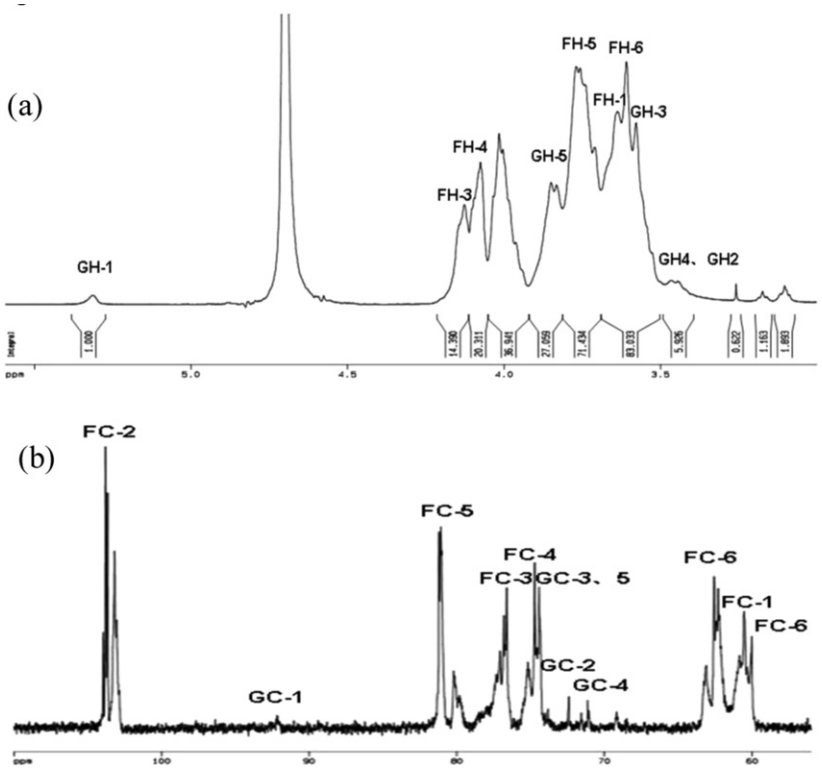

Fig. 4. 1D NMR spectrum of GF in D_2O (a) ^1H NMR spectrum; (b) ^{13}C NMR spectrum.

^1H resonances for H-1, H-2, H-3, H-4 of residue **a** (Table 1) were assigned from the cross-peakes in the ^1H–^1H COSY spectrum (Fig. 5b). H-5, H-6a and H-6b of residue **a** (Table 1) were assigned from the ^1H–^1H COSY and HMBC (Fig. 5c) spectrums. The carbon chemical shifts from the C-1 to C-6 of residue **a** (Table 1) were assigned from the HSQC spectrum (Fig. 5a). The downfield shift of the C-6 (δ 62) carbon signal relative to standard values for glycopyrannoses and the H-1 at δ 5.31 ppm indicated that residue **a** (Table 1) was α-D-*Glc*-(1 → (Matulova, Husarova, Capek, Sancelme, & Delort, 2011).

The ^1H resonances for H-1, H-3, H-4 of residue **b**, **c**, **d**, and **e** (Table 1) were assigned from ^1H–^1H COSY spectrum, and the assignment of H-5, H-6 were assigned from the ^1H–^1H COSY and HMBC spectrums (Fig. 5). On basis of the proton assignments, C-1 to C-6 were readily obtained from the HSQC and HMBC spectrums. The signal at δ 103.2 of Fru*f* was typical for C-2 of a (2 → 1)-linked residue (Table 1 **b**) (Matulova et al., 2011). The signals at δ 103.6 (Table 1 **c**) and 103.8 (Table 1 **d**) of Fru*f* were assigned to terminal and branched residues, respectively. And that at δ 103.9 of Fru*f* was assigned to a (2 → 6)-linked residue (Table 1 **e**). Thus, the four residues of Fru*f* were identified as →1)-Fru*f*-(2→, →1,6)-Fru*f*-(2→, Fru*f*-(2→, →6)-Fru*f*-(2→, respectively.

Our NMR results showed that the structure of GF from white garlic was consistent with the fructan from aged garlic (Chandrashekar et al., 2011). The main chain of GF was primarily composed of (2 → 1)-β-D-fructopyranose, linked to a terminal (2 → 1)-α-D-glucopyranose at the non-reducing end and (2 → 6)-β-D-fructopyranose branching on its backbone. However, it was different from the findings of Baumgartner et al. (2000), who reported that fructan from garlic had a (2 → 1)-linked β-D-fructopyranose backbone with (2 → 6)-linked β-D-fructopyranose side chains and an α-D-glucopyranose (1 → 6) linkage.

3.2. Effect of GF on the viability of UVB-exposed cells

According to the MTT assay data (Fig. 6), increasing concentrations of GF substantially increased cell viability, compared to cells absent GF and UVB ($p < 0.05$). Cell viability decreased rapidly, 12 h

Table 1
Chemical shifts data for GF isolated from white garlic.

Residue		Proton or carbon					
		1	2	3	4	5	6
α-D-*Glc*-(1 → (**a**)	H	5.31	3.46	3.58	3.44	3.85	–
	C	92.2	71.1	72.4	69.2	71.6	–
→1)-*Fruf*-(2 → (**b**)	H	3.76/3.61		4.09	4.01	3.77	3.71/3.58
	C	60.5	103.2	77.1	75.2	81.1	62.6
→1,6)-*Fruf*-(2 → (**c**)	H	3.96/3.85		4.12	4.07	3.61	3.77/3.74
	C	60.6	103.6	77.4	74.9	81.2	62.4
Fruf-(2 → (**d**)	H	3.76/3.71		4.03	3.85	3.64	3.10/3.01
	C	61.7	103.8	78.1	74.8	80.2	62.8
→6)-*Fruf*-(2 → (**e**)	H	3.83/3.77		4.02	3.96	3.61	3.78/3.73
	C	60.5	103.9	76.8	75.9	81.2	62.0

All values are given as chemical shifts in ppm; –: overlap of signals or without signals.

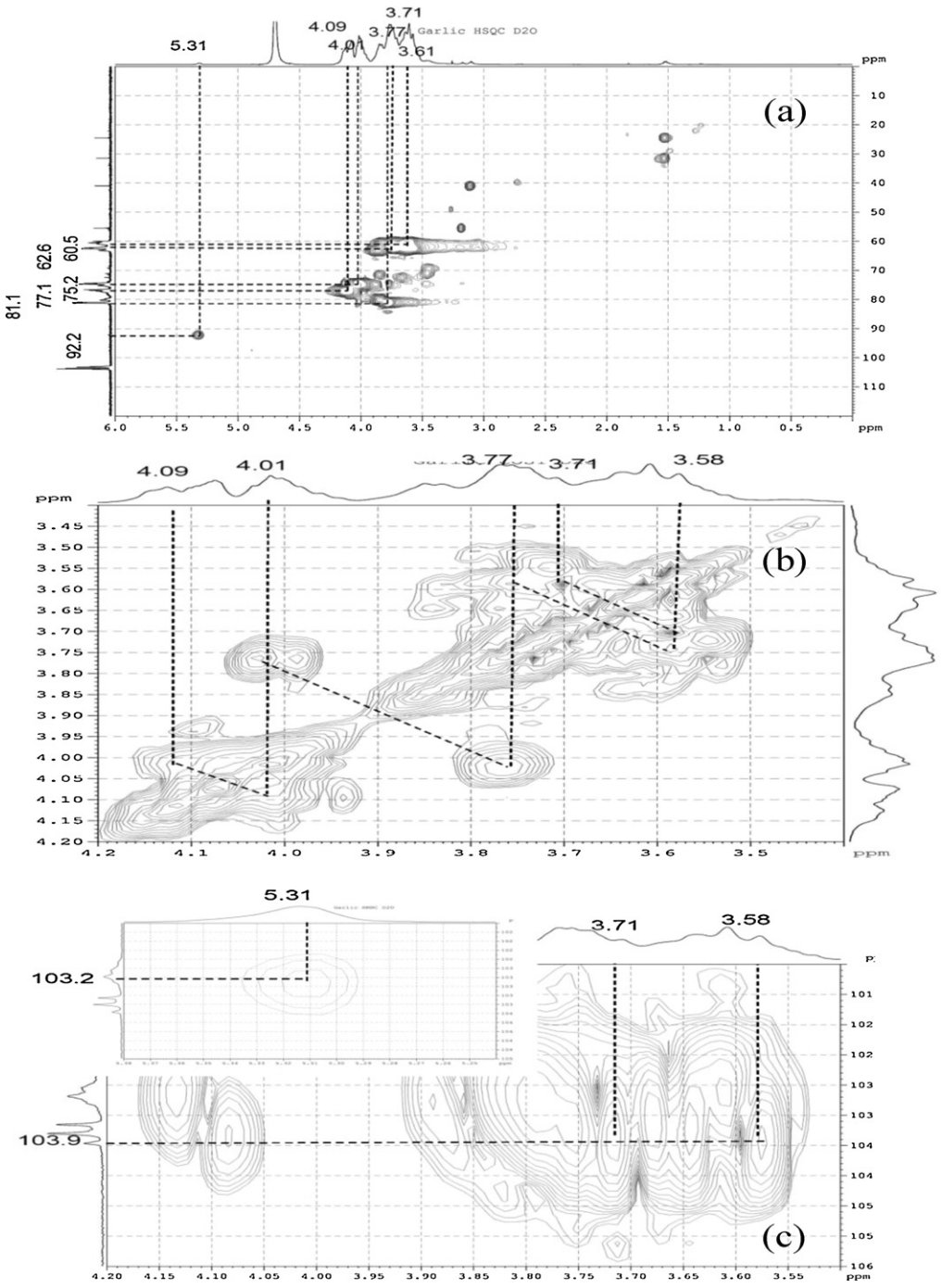

Fig. 5. 2D NMR spectrum of GF in D_2O (a) HSQC spectrum of GF; (b) COSY spectrum of GF; (c) HMBC spectrum of GF.

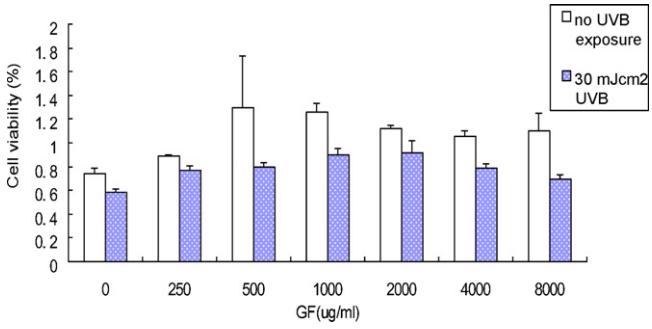

Fig. 6. Effect of GF on the viability of UVB-exposed cells. Values are expressed as means ± SD ($n = 6$), $p < 0.05$.

after UVB exposure with energy 30 mJ/cm^2 ($p < 0.05$). Exposure of cells to increase concentrations of GF substantially increased cell viability compared to UVB-exposed cells. The MTT assay revealed that the presence of GF effectively decreased the degree of cell injury following UVB exposure.

3.3. Effect of GF on UVB-induced sub-G1 cell cycle arrest

UVB exposed cells in the absence or presence of GF were analyzed to determine its influence on the cell cycle. As shown in Fig. 7, the sub-G1 phase was significantly lengthened in UVB (30 mJ/cm^2) exposed cells compared to non-exposed cells ($p < 0.05$), whereas

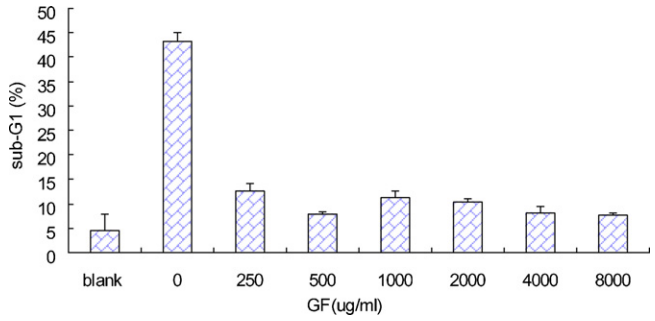

Fig. 7. Effect of GF on UVB-induced sub-G1 cell cycle arrest. Values are expressed as means ± SD ($n = 3$), $p < 0.05$.

the percentage of cells in the sub-G1 phase was decreased following GF treatment.

4. Conclusions

One purified polysaccharide with a yield of 6.15% (w/w) was obtained from white garlic and identified. It appeared that the average MW of GF was 4.5×10^3 Da. After acid hydrolysis of GF, HPAEC analysis showed that GF was composed of fructosyl and glycosyl units at a ratio of 14:1. An NMR spectrum confirmed that the GF was 1-kestose-type fructan, and that it had a backbone of $(2 \rightarrow 1)$ linked β-D-Fru*f*, ending with a $(2 \rightarrow 1)$ linked α-D-Glcp residue, while the side chain was $(2 \rightarrow 6)$-linked-β-D-Fru*f*. Moreover, GF significantly protected human keratinocytes from UVB induced damage ($p < 0.05$). The efficacy of GF in this regard provides evidence that this functional plant extract may be developed as a novel antioxidant. The correlation between structure and function needs further confirmation.

Acknowledgments

We are grateful for the financial support of the China National Natural Science Foundation (No. 31171722) and Special Fund for Agro-Scientific Research in the Public Interest (200903018). The technical writing supported by Dr. William W. Riley, Jinan University (Guangzhou, China) is acknowledged.

References

Baumgartner, S., Dax, T. D., Praznik, W., & Falk, H. (2000). Characterisation of the high-molecular weight fructan isolated from garlic (*Allium sativum* L.). *Carbohydrate Research*, *328*, 177–183.

Chandrashekar, P. M., Harish Prashanth, K. V., & Venkatesh, Y. P. (2011). Isolation, structural elucidation and immunomodulatory activity of fructans from aged garlic extract. *Phytochemistry*, *72*, 255–264.

Chen, Q., Zhang, S. Z., Ying, H. Z., Dai, X. Y., Li, X. X., Yu, C. H., et al. (2012). Chemical characterization and immunostimulatory effects of a polysaccharide from *Polygoni Multiflori Radix Praeparata* in cyclophosphamide-induced anemic mice. *Carbohydrate Polymers*, *88*, 1476–1482.

Chen, Z. L., Cao, G. Q., & Song, Q. J. (2010). Photo-polymerization of triclosan in aqueous solution induced by ultraviolet radiation. *Environmental Chemistry Letters*, *8*, 33–37.

Cipriani, T. R., Mellinger, C. G., Souza, L. M. D., Baggio, C. H., Freitas, C. S., Marques, M. C. A., et al. (2006). A polysaccharide from a tea (Infusion) of *Maytenus ilicifolia* leaves with anti-ulcer protective effects. *Journal of Natural Products*, *69*, 1018–1021.

Hsiao, G., Shen, M. Y., Lin, K. H., Lan, M. H., Wu, L. Y., Chou, D. S., et al. (2003). Antioxidative and hepatoprotective effects of antrodia camphorata extract. *Journal of Agricultural and Food Chemistry*, *51*, 3302–3308.

Huang, X. S., & Chen, J. L. (2011). Effect of different fractions of garlic fructan on lactic fermentability. In *International conference on agricultural and biosystems engineering* Hong Kong, Peoples Republic of China, (pp. 262–265).

Kippenberger, S., Loitsch, S. M., Grundmann-Kollmann, M., Simon, S., Dang, T. A., Hardt-Weinelt, K., et al. (2001). Activators of peroxisome proliferator-activated receptors protect human skin from ultraviolet-B-light-induced inflammation. *Journal of Investigative Dermatology*, *117*, 1430–1436.

Liu, S. C., Mizu, H., & Yamauchi, H. (2007). Molecular response to phototoxic stress of UVB irradiated ketoprofen through arresting cell cycle in G2/M phase and inducing apoptosis. *Biochemical and Biophysical Research Communications*, *364*, 650–655.

Losso, J. N., & Nakai, S. (1997). Molecular size of garlic fructooligosaccharides and fructopolysaccharides by matrix-assisted laser desoportion ionization mass spectrometry. *Journal of Agriculture and Food Chemistry*, *45*(11), 4342–4346.

Luo, Q., Sun, Q., Wu, L. S., & Yang, Z. R. (2012). Structural characterization of an immunoregulatory polysaccharide from the fruiting bodies of *Lepista sordida*. *Carbohydrate Polymers*, *88*, 820–824.

Masuko, T., Minami, A., Iwasaki, N., Majima, T., Nishimura, S. I., & Lee, Y. C. (2005). Carbohydrate analysis by a phenol–sulfuric acid method in microplate format. *Analytical Biochemistry*, *339*, 69–72.

Matulova, M., Husarova, S., Capek, P., Sancelme, M., & Delort, A. M. (2011). NMR structural study of fructans produced by *Bacillus* sp. 3B6, bacterium isolated in cloud water. *Carbohydrate Research*, *346*, 501–507.

Nguyen, T. A., Do, T. T., Nguyen, T. D., Pham, L. D., & Nguyen, V. D. (2011). Isolation and characteristics of polysaccharide from *Amorphophallus corrugatus* in Vietnam. *Carbohydrate Polymers*, *84*, 64–68.

Politi, M., Alvaro-Blanco, J., Groves, P., Prieto, A., Leal, J. A., Canada, F. J., et al. (2006). Screening of garlic water extract for binding activity with cholera toxin B pentamer by NMR spectroscopy – An old remedy giving a new surprise. *European Journal of Organic Chemistry*, *9*, 2067–2073.

Praznik, W., Huber, A., & Cieslik, E. (2004). Fructans: Occurrence and application in food. In P. Tomasik (Ed.), *In chemical and functional properties of food saccharides*. Boca Raton, USA: CRC Press, pp. 211–211.

Shi, S. M., Yan, R. A., Li, Y. S., & Huang, X. S. (2008). Studies on the antioxidation activity of garlic polysaccharide. *Food Science and Technology*, *9*, 169–173.

Sitailo, L. A., Tibudan, S. S., & Denning, M. F. (2002). Activation of Caspase-9 is required for UV-induced apoptosis of human keratinocytes. *The Journal of Biological Chemistry*, *277*, 19346–19352.

Tong, H. B., Liang, Z. Y., & Wang, G. Y. (2008). Structural characterization and hypoglycemic activity of a polysaccharide isolated from the fruit of *Physalis alkekengi* L. *Carbohydrate Polymers*, *71*, 316–323.

Tsukamoto, S., Okamoto, K., Inanaga, J., & Karasaki, Y. (2008). Purification, characterization and biological activities of a garlic oligosaccharide. *Journal of UOEH*, *30*, 147–157.

Yang, L., & Zhang, L. M. (2009). Chemical structural and chain conformational characterization of some bioactive polysaccharides isolated from natural sources. *Carbohydrate Polymers*, *76*, 349–361.

Zeng, W. C., Zhang, Z., Gao, H., Jia, L. R., & Chen, W. Y. (2012). Characterization of antioxidant polysaccharides from *Auricularia auricular* using microwave-assisted extraction. *Carbohydrate Polymers*, *89*(2), 694–700.

Zhang, A. Q., Xiao, N. N., Deng, Y. L., He, P. F., & Sun, P. L. (2012). Purification and structural investigation of a water-soluble polysaccharide from *Flammulina velutipes*. *Carbohydrate Polymers*, *87*, 2279–2283.